Immunity, Vol. 7, 419–432, September, 1997, Copyright ©1997 by Cell Press

Listeriosis in *p47$^{phox-/-}$* and *TRp55$^{-/-}$* Mice: Protection Despite Absence of ROI and Susceptibility Despite Presence of RNI

Robert Endres,* Arne Luz,† Helga Schulze,† Hans Neubauer,* Agnes Fütterer,* Steven M. Holland,‡ Hermann Wagner,* and Klaus Pfeffer*§

*Institute for Medical Microbiology, Immunology and Hygiene
Technical University of Munich
Trogerstrasse 9
D-81675 Munich
Federal Republic of Germany
†Institute of Pathology
GSF-National Research Center for Environment and Health
Ingolstädter Landstrasse 1
D-85758 Oberschleissheim
Federal Republic of Germany
‡Laboratory of Host Defenses
National Institutes of Allergy and Infectious Diseases
National Institutes of Health
Bethesda, Maryland 20892–1886

Summary

The significance of host defense mechanisms in primary listeriosis in vivo is incompletely understood. Here, we show that tumor necrosis factor receptor p55$^{-/-}$ (*TRp55$^{-/-}$*) mice are susceptible to Listeria monocytogenes infection in the presence of leukocyte recruitment, inflammatory cytokine production (including IFNγ), nitric oxide synthesis, and oxidative burst formation. Mice deficient for oxidative burst (*p47$^{phox-/-}$* mice) are relatively resistant to listeriosis. Despite activation of these antibacterial effector systems, *TRp55$^{-/-}$* phagocytes in vivo are incapable of confining and eradicating L. monocytogenes inside phagolysosomes. Bone marrow chimeras reveal that for eradication of L. monocytogenes, TRp55 is crucially required only on cells from hematopoietic origin. Unexpectedly, prior to death, exocrine pancreatic cells undergo apoptosis in *TRp55$^{-/-}$* mice. Collectively, these data demonstrate that in vivo, TRp55 initiates a protective, listericidal mechanism in phagocytes that differs from nitric oxide production and oxidative burst formation and that uncontrolled listeriosis results in necrotizing pancreatitis in *TRp55$^{-/-}$* mice.

Introduction

In recent years, gene-targeted mice have proven instrumental for the definition of molecular host components that are essential for the survival of an infection with intracellular bacteria. Thus, inoculation of minute amounts of Listeria monocytogenes into mice rendered deficient for genes such as the tumor necrosis factor (TNF) receptor p55 gene (Pfeffer et. al., 1993; Rothe et al., 1993), the interferon-γ (IFNγ) and IFNγ-receptor genes (Huang et al., 1993; Harty and Bevan, 1995), the interferon consensus sequence binding protein gene (Fehr et al., 1997), or the nuclear factor (NF)–interleukin-6 (IL-6) gene (Tanaka et al., 1995) is detrimental for these animals. The molecular and cellular mechanisms ultimately leading to this marked immunoincompetence are so far only poorly understood.

Infection with L. monocytogenes, a facultatively intracellular, gram-positive rod, has served extensively as a model system for the investigation of host defense mechanisms. In the immunocompetent host, protective immunity against L. monocytogenes evolves through several phases, each of which is controlled by different cell types and cytokines (Kaufmann, 1993; Harty et al., 1996; Unanue, 1997). Infection due to L. monocytogenes requires for its early control the nonspecific or innate immune response and, subsequently, for final eradication of bacteria, the specific cellular immune response (Bancroft et al., 1991; Harty et al., 1996). One of the initial mechanisms of resistance is phagocytosis and breakdown of most bacteria by resident macrophages such as Kupffer cells in the liver (Rosen et al., 1989; Portnoy, 1992). This is followed by the rapid recruitment of neutrophils (day 1) to the sites of bacterial infection (Mandel and Cheers, 1980; Portnoy, 1992). The presence of neutrophils is pivotal during the early stages (0–48 hr) of L. monocytogenes infection (Conlan and North, 1991, 1994; Rogers and Unanue, 1993). Also early in listeriosis, natural killer (NK) cells are activated. At this time, NK cells are the major source of IFNγ (Dunn and North, 1991; Teixeira and Kaufmann, 1994), a cytokine that is crucially required for the complete arming of phagocytes (Portnoy, 1992). From days 2–4, monocytes and macrophages infiltrate the sites of infection and contribute to the formation of early granulomatous lesions that are composed of granulocytes and, mainly, activated macrophages (Mandel and Cheers, 1980). The end of the innate phase is marked by an influx of T cells to the sites of infection on days 4–5 (Goosens et al., 1991). If innate immune defenses are persisting at that time, the acquired immune response will then be able to mediate the eventual clearance of L. monocytogenes via specific T cell responses (Bancroft et al., 1991; Kaufmann, 1993; Harty et al., 1996).

A key cytokine being immediately necessary for survival after infection with L. monocytogenes is TNFα (Nakane et al., 1988; Havell, 1989). The effects of TNFα are mediated via two distinct cell surface receptors, TNF receptor p55 (TRp55) and p75 (TRp75). Mice rendered deficient in the *TRp55* gene rapidly succumb to infection by L. monocytogenes (Pfeffer et al., 1993; Rothe et al., 1993) or mycobacteria (Flynn et al., 1995), proving that signals mediated by TRp55 are essential for the antibacterial effects of TNFα. Several hypotheses for explaining the mechanism by which TNFα exerts its beneficial effects have been put forward. TNFα was suggested to be an important factor for chemotaxis or focusing of phagocytic cells within sites of L. monocytogenes infection (Havell, 1989) and to play a pivotal role in the formation of granulomas during an infection with bacillus Calmette-Guerin (Kindler et al., 1989). In addition, the

§To whom correspondence should be addressed.

hypothesis exists that TNFα acts directly to lyse infected hepatocytes (Portnoy, 1992). In vitro, TNFα and IL-12 can synergize on the production of IFNγ by NK cells (Tripp et al., 1993, 1994). Moreover, TNFα in concert with IFNγ efficiently enhances the formation of an oxidative burst reaction in murine peritoneal exudate macrophages (Ding et al., 1988). TNFα was also demonstrated to be capable of directly stimulating adherent human granulocytes for the production of reactive oxygen intermediates (ROI) (Clatham et al., 1994). In vivo, ROI are involved in the control of extracellular bacteria such as staphylococci (Jackson et al., 1995). In macrophages in vitro, production of nitric oxide (NO) as a result of the expression of inducible nitric oxide synthase (iNOS) is strongly induced by TNFα in synergy with IFNγ (Ding et al., 1988). Yet still there is controversial evidence about the requirement for reactive nitrogen intermediates (RNI) in the process of L. monocytogenes elimination in vivo (Beckerman et al., 1993; Leenen et al., 1994; MacMicking et al., 1995; Fehr et al., 1997).

Here, in vivo evidence is provided that, despite influx of inflammatory cells to the sites of infection, despite up-regulation of effector cytokines, and despite production of ROI and RNI, *TRp55*-deficient phagocytes are incapable of controlling intracellular L. monocytogenes replication. However, substantial numbers of exocrine pancreatic cells ultimately undergo apoptosis in *TRp55*$^{-/-}$ mice. Moreover, in *p47*$^{phox-/-}$ mice, oxidative burst formation per se is demonstrated to play only a minor role in the anti–L. monocytogenes host defense.

Results

L. monocytogenes Infection in *TRp55*$^{-/-}$, *p47*$^{phox-/-}$, and Bone Marrow Chimeric Mice

TRp55$^{-/-}$ mice readily die as a result of L. monocytogenes infection (Pfeffer et al., 1993; Rothe et al., 1993). To determine the degree of susceptibility of *TRp55*$^{-/-}$ mice to an L. monocytogenes challenge, the infection dosage was titrated (Figure 1A). *TRp55*$^{-/-}$ mice could not resist a dosage of 500 colony-forming units (cfu) of inoculated L. monocytogenes, which is 1:1000 of the 50% lethal dose (LD_{50}) for syngeneic C57BL/6 control mice. The time point of death ranged from 3 days (5×10^5 L. monocytogenes intraperitoneally) to 7 days (5×10^2 L. monocytogenes intraperitoneally), respectively. These data indicate that *TRp55*$^{-/-}$ mice are extremely sensitive to L. monocytogenes infection. In the next set of experiments, the spread and growth of L. monocytogenes in liver, spleen, pancreas, and brain were analyzed during the course of infection. Almost exponential bacterial growth took place in the livers of *TRp55*$^{-/-}$ mice up to the time of death (Figure 1B). In contrast, in control mice, after an initial rapid increase, L. monocytogenes colony-forming units reached a plateau 72 hr postinfection and declined thereafter. Twenty-four hours, 72 hr, and 96 hr postinfection, approximately 10-, 30-, and 1000-fold more colony- forming units, respectively, could be recovered from *TRp55*$^{-/-}$ than from *TRp55*$^{+/+}$ livers (Figure 1B). Comparable kinetics were observed in spleen and pancreas (Figure 1B). Of note, the brain of *TRp55*$^{-/-}$ mice did not appear to be a primary target organ since bacterial numbers were consistently three orders of magnitude lower than in peripheral organs (Figure 1B). To further address the question of whether the presence of TRp55 is pivotal on immune cells and/or nonhematopoietically derived cells (e.g., hepatocytes) during listeriosis, infection experiments on radiation bone marrow (BM) chimeric mice were performed. *TRp55*$^{-/-}$ BM→C57BL/6, C57BL/6 BM→*TRp55*$^{-/-}$, and control C57BL/6 BM→C57BL/6 mice were produced and subsequently infected with titrated amounts of L. monocytogenes. In contrast to C57BL/6 BM→*TRp55*$^{-/-}$ and control C57BL/6 BM→C57BL/6 chimeras, *TRp55*$^{-/-}$ BM→C57BL/6 chimeras were highly susceptible to listeriosis (Figure 1A). Taken together, these findings demonstrate the crucial dependence for TRp55 on cells from hematopoietic origin, but not on nonhematopoietically derived cells such as hepatocytes, to curb growth of L. monocytogenes during the innate phase of the host immune defense.

Recruitment of Inflammatory Cells

Currently, it is unclear why *TRp55*$^{-/-}$ mice cannot control L. monocytogenes replication in vivo. TNFα and TRp55 are involved in the up-regulation of a set of adhesion molecules (Bevilacqua, 1993; Neumann et al., 1996). Therefore, we addressed the question of whether mice lacking *TRp55* might be deficient to recruit inflammatory cells to the place of bacterial infection. *TRp55*$^{-/-}$ and control mice were infected with 5×10^4 L. monocytogenes organisms intraperitoneally; livers were removed 24 and 72 hr postinfection; and the influx of granulocytes and monocytes was monitored by immunohistochemical analysis of cryosections. Twenty-four hours postinfection, granulocytes (Gr-1$^+$/Mac-1$^+$) could be detected in small clusters scattered throughout the liver parenchyma of both *TRp55*$^{-/-}$ mice and control mice (Figure 2). The number of these clusters was slightly reduced in homozygous-mutant mice. As described previously for wild-type mice (Mandel and Cheers, 1980), 72 hr postinfection in control mice, early granulomatous lesions had formed consisting of Gr-1$^+$/Mac-1$^+$ granulocytes and Gr-1$^-$/Mac-1$^+$ monocytes or macrophages. Unexpectedly, the cellular composition and the number of granulomatous lesions in *TRp55*$^{-/-}$ animals were not significantly different from control mice at this time point (Figure 2). This result was confirmed by examination of hematoxylin–eosin–stained paraffin sections (data not shown). In accordance with previous findings (Goosens et al., 1991), immunohistochemistry further revealed that CD4 and CD8 antigen–positive T cells did not infiltrate into livers of L. monocytogenes–infected mice in significant numbers during the first 72 hr. In summary, recruitment of inflammatory cells with a neutrophilic first phase followed by a monocyte or macrophage invasion that is accompanied by formation of granulomatous lesions appeared grossly unaltered in *TRp55*$^{-/-}$ mice. These data suggest that in vivo, for the attraction of cells of the innate immune response, signaling via the TRp55 can be largely compensated by alternative signaling pathways.

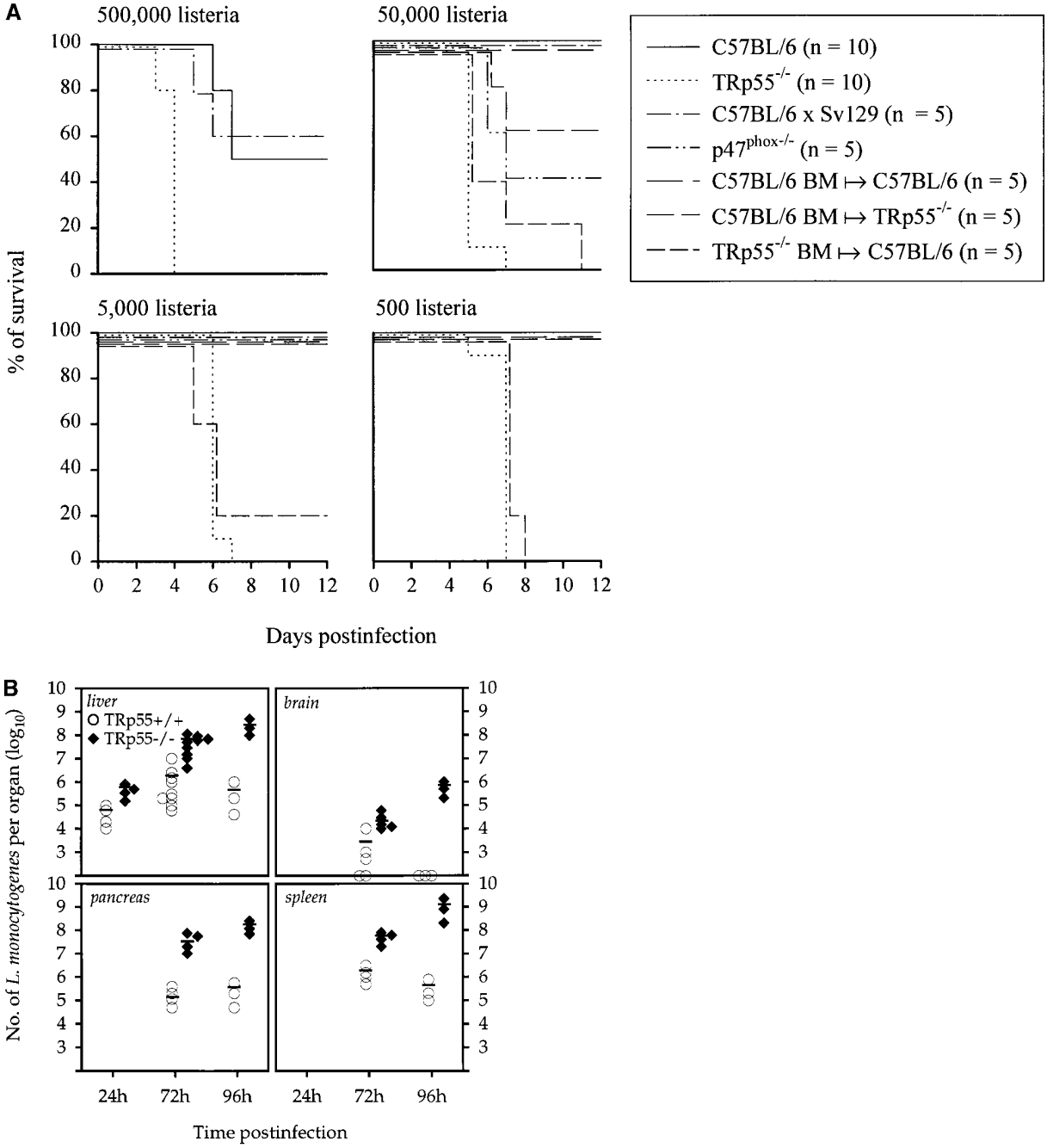

Figure 1. Survival Kinetics (A) and Bacterial Counts (B) after L. monocytogenes Infection

(A) Survival kinetics of *TRp55*$^{-/-}$ mice, syngenic C57BL/6 control mice, *p47*^{phox} −/− mice, C57BL/6 × Sv129 control mice, *TRp55*$^{-/-}$ BM→C57BL/6 chimeras, C57BL/6 BM→*TRp55*$^{-/-}$ chimeras, and control C57BL/6 BM→C57BL/6 chimeras. Mice were infected intraperitoneally with the indicated amounts of viable L. monocytogenes (strain ATCC 43251) at day 0. Mice still alive on day 12 postinfection showed no signs of illness during the rest of the observation period (day 20 postinfection).

(B) Bacterial load after L. monocytogenes infection in different tissues of *TRp55*$^{-/-}$ mice. Animals (each symbol represents one mouse) were infected with 5×10^4 viable L. monocytogenes intraperitoneally. Numbers of bacteria were determined at indicated time points by plating tissue homogenates in 10-fold serial dilutions on Columbia blood agar plates.

Cellular and Subcellular Localization of L. monocytogenes

Previous in vitro experiments suggested that TNFα plays an important role for control of L. monocytogenes growth inside macrophages (Portnoy et al., 1989; Leenen et al., 1994). To determine whether *TRp55*-deficient phagocytes were capable of controlling L. monocytogenes replication in vivo, the cellular and subcellular localization of bacteria was examined. Twenty-four hours postinfection, hardly any L. monocytogenes were detectable

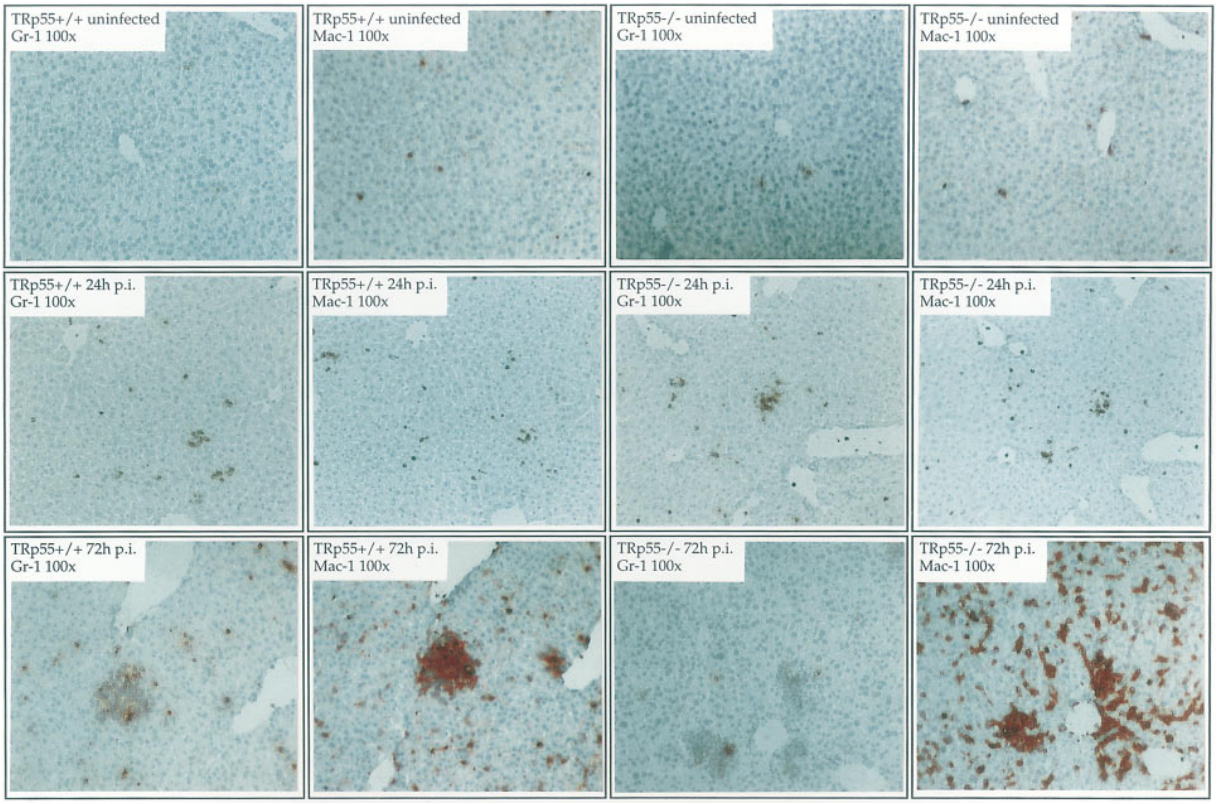

Figure 2. Recruitment of Inflammatory Cells and Formation of Granulomatous Lesions

Mice ($n \geq 6$ per group) were infected with 5×10^4 L. monocytogenes intraperitoneally or left untreated. Livers were removed from uninfected mice (top lane) or from infected mice after 24 hr (middle lane) or 72 hr (bottom lane). Cryosections were prepared and examined by immunohistochemistry. For genotype of mice, antigens stained, and original magnifications, refer to inserts. Representative sections from one mouse per group are shown. p.i., postinfection.

within livers of *TRp55*$^{-/-}$ or control mice (data not shown). However, 72 hr postinfection, in liver sections of *TRp55*$^{-/-}$ mice, L. monocytogenes could be easily visualized inside granulomatous lesions (Figure 3A). Ninety-six hours postinfection, L. monocytogenes were detected both inside granulomatous lesions and, in addition, in some heavily infected cells nearby granulomatous lesions (Figure 3A). In contrast, granulomatous lesions of control mice contained only a few or no detectable L. monocytogenes (Figure 3A). To further clarify the cellular and subcellular localization of L. monocytogenes, electron microscopic examination of granulomatous lesions and the surrounding liver parenchyma was performed. Ninety-six hours postinfection, many phagocytes containing L. monocytogenes could be observed inside granulomatous lesions of *TRp55*$^{-/-}$ mice (Figure 3B and Table 1). In accordance with light microscopy, some heavily infected hepatocytes were encountered at the periphery of granulomatous lesions (Figure 3B and Table 1). L. monocytogenes organisms in hepatocytes were not surrounded by host cell membranes and appeared free in the cytoplasm. In phagocytes of *TRp55*$^{-/-}$ animals, ~70% of the L. monocytogenes resided in single- or multilayer membrane vacuoles, and ~30% were found free in the cytoplasm (Figure 3B). Multilayer membrane vacuoles are believed to form around L. monocytogenes during active spread from one host cell to another (Racz et al., 1970). In homozygous-mutant mice, almost all L. monocytogenes were found ultrastructurally intact, indicating viability of bacteria. In contrast, in livers of control mice, only very few intact L. monocytogenes were detectable by electron microscopy 96 hr postinfection (Table 1). However, some phagocytes contained electron-dense debris in vacuoles possibly representing remnants of digested L. monocytogenes (data not shown). Taken together, the presence of many ultrastructurally intact L. monocytogenes, some of which were even replicating and/or free in the cytoplasm, provides evidence that *TRp55*-deficient phagocytes are incapable of controlling L. monocytogenes replication.

Oxidative Burst Formation

Generation of ROI (oxidative burst) as a major bactericidal mechanism in granulocytes and macrophages has been widely studied (Lepay et al., 1985; Peck, 1989). However, the in vivo importance of an oxidative burst formation for the clearance of an L. monocytogenes infection is still not clearly defined. Gene-targeted *p47*$^{phox-/-}$ mice, which are unable to produce ROI (Jackson et al., 1995), therefore were infected with titrated amounts of L. monocytogenes. In contrast to *TRp55*$^{-/-}$ mice, the LD_{50} for *p47*$^{phox-/-}$ animals (C57BL/6 × Sv129 background) was determined to be only one order of

Table 1. Cellular Localization of L. monocytogenes in the Liver as Determined by Electron Microscopy 96 hr Postinfection

	TRp55$^{+/+}$	*TRp55*$^{-/-}$
Number of granulomatous lesions examined	8	8
Number of infected phagocytes	3	156
Range of listeria number in infected phagocytes (mean number ± SD)	1	1–5 (2 ± 1.5)
Number of infected hepatocytes	0	24
Range of listeria number in infected hepatocytes (mean number ± SD)	—	3–30 (9 ± 8)

magnitude below that of C57BL/6 × Sv129 control mice (Figure 1A), indicating that lack of an oxidative burst formation does not render mice highly susceptible to listeriosis. In a second set of experiments, *TRp55*-deficient and wild-type granulocytes from uninfected and infected mice were analyzed with respect to their capacity to respond with ROI formation after activation. Whole blood was taken from uninfected mice or 24 hr postinfection. After lysis of erythrocytes, cells were loaded with dihydrorhodamine 123 dye and stimulated with N-formyl-methionyl-leucyl-phenylalanine (fMLP). Oxidative burst formation was monitored by flow cytometry. Degranulation of granulocytes indicated by a reduction of side scatter signals occurred similarly in uninfected and infected *TRp55*$^{-/-}$ and control mice after fMLP stimulation (data not shown). Interestingly, the percentage of cells in the granulocyte gate significantly increased in infected animals versus uninfected animals (*TRp55*$^{-/-}$ mice, 34.9% ± 10.5% versus 7.8% ± 2.0%; control mice, 40.3% ± 4.8% versus 9.5% ± 2.1%; $p < 0.05$, $n = 6$

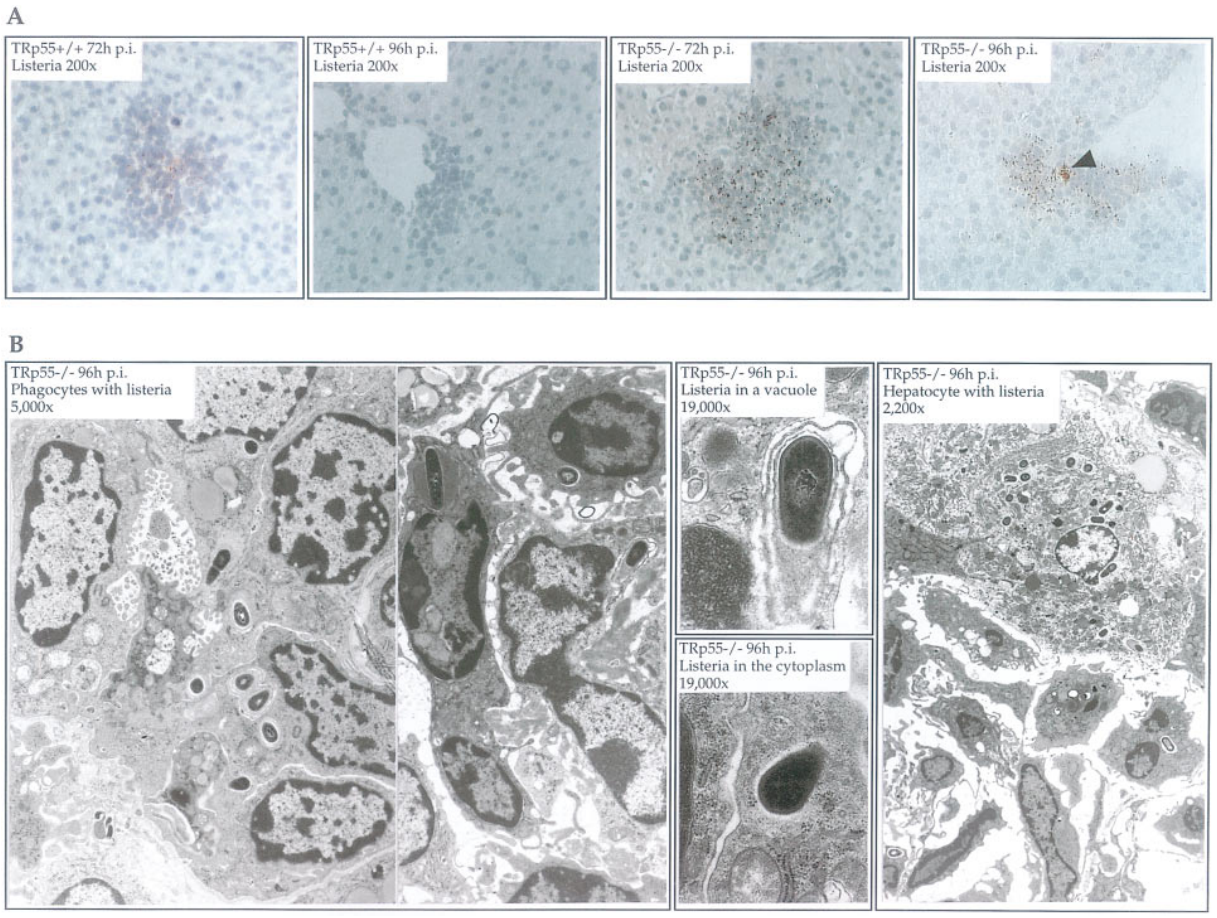

Figure 3. Localization of L. monocytogenes inside the Liver

Mice ($n \geq 5$ per group) were infected with 5×10^4 L. monocytogenes intraperitoneally.

(A) Livers were removed 72 hr and 96 hr postinfection. Immunohistochemistry was performed on cryosections. Polyclonal rabbit serum raised against L. monocytogenes was used as primary antibody for immunodetection of the bacteria. For genotype of mice, antigens stained, and original magnifications, refer to inserts. Note the heavily infected single cell possibly representing an infected hepatocyte (arrowhead).

(B) Livers were removed 96 hr postinfection, and electron microscopic examination of granulomatous lesions was carried out on sections of control mice (data not shown) and *TRp55*$^{-/-}$ mice. For explanations and magnifications, refer to inserts. Representative sections are shown. Note that at 5000× magnification, two independent micrographs are presented.

per group). Moreover, significantly higher mean fluorescence intensities demonstrated that oxidative burst formation was increased in granulocytes from infected *TRp55*$^{-/-}$ and control mice as compared to granulocytes from naive mice (Figure 4; $p < 0.05$; $n = 6$ per group). No significant differences could be found in the capacity of ROI generation between naive *TRp55*$^{-/-}$ and naive control mice and between infected *TRp55*$^{-/-}$ and infected control mice. Collectively, these data show first, that during listeriosis, induction of a comparable blood neutrophilia occurs in *TRp55*$^{-/-}$ and control mice, and second, that the absence of listericidal activity in *TRp55*-deficient phagocytes cannot be ascribed to a lack of ROI production.

Up-Regulation of Inflammatory Cytokines in Liver and Serum

The incompetence of phagocytes to kill L. monocytogenes might be due to impaired induction of inflammatory cytokines that are crucial for full bactericidal activity of phagocytes. In this regard, IFNγ is considered to be a potent activator of antibacterial effector functions in phagocytes (Buchmeier and Schreiber, 1985; Bancroft et al., 1991). One day after L. monocytogenes infection, NK cells appear to be the major source of IFNγ (Dunn and North, 1991; Teixeira and Kaufmann, 1994). In vitro studies demonstrated an antagonistic effect of IL-10 (Tripp et al., 1993) and an agonistic effect of TNFα and IL-12 on the production of IFNγ by NK cells (Tripp et al., 1993, 1994). Therefore, in *TRp55*$^{-/-}$ animals, a different expression pattern of these cytokines could ultimately result in a diminished production of IFNγ. A sensitive, semiquantitative, internal-competitive reverse transcription–polymerase chain reaction (RT–PCR) approach was chosen to evaluate this hypothesis. The kinetics of IL-10, IL-12, TNFα, and IFNγ mRNA expression in liver tissue of *TRp55*$^{-/-}$ and control mice were investigated. Surprisingly, 24 hr postinfection, significant differences in the up-regulation or in the amounts of cytokine mRNAs (IL-10, IL-12, TNFα, and IFNγ) between homozygous-mutant and control mice could not be observed (Figure 5A). Similar results were obtained for IFNγ mRNA determined 72 hr postinfection. In addition, enzyme-linked immunosorbent assay (ELISA) measurements of TNFα and IFNγ in the serum of infected mice revealed comparable amounts of IFNγ and TNFα circulating in the serum 24 hr postinfection (Figure 5B). Seventy-two hours and 96 hr postinfection, serum concentrations of TNFα and IFNγ in *TRp55*$^{-/-}$ mice even exceeded those of control mice (Figure 5B), whereas IL-1β amounts were not significantly different on day 3 (16 ± 5 pg/ml versus 17 ± 7 pg/ml; $n = 5$ per group). Taken together, the defective bactericidal activity of phagocytes in *TRp55*$^{-/-}$ mice cannot be attributed to a dysregulation of IL-10 or a diminished production of IL-12 or IFNγ. Moreover, primary activation of NK cells as characterized by early IFNγ production does not crucially depend on the presence of TRp55.

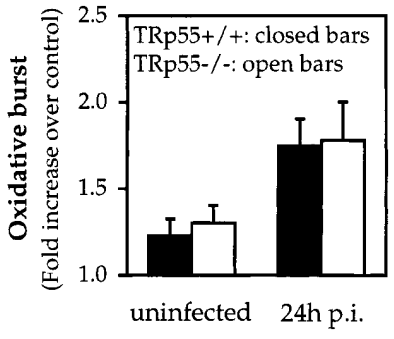

Figure 4. Oxidative Burst Formation in Uninfected and L. monocytogenes–Infected Mice

Comparison of oxidative burst formation in *TRp55*$^{-/-}$ and *TRp55*$^{+/+}$ granulocytes derived from naive mice or from mice infected intraperitoneally with 5×10^4 L. monocytogenes organisms 24 hr earlier. Dihydrorhodamine 123–loaded granulocytes were treated with control medium or fMLP for 20 min at 37°C. The mean fluorescence channel of each treatment was standardized to the control medium and shown as the fold increase over control. The mean ± SEM for six mice is shown.

Activation Status of Recruited Inflammatory Cells

Since NK cell activation occurs appropriately in *TRp55*$^{-/-}$ animals, the activation status of recruited macrophages was addressed. Expression of major histocompatibility complex (MHC) class II and the induction of IFNγ-responsible genes such as macrophage activation gene-1 (*mag-1*) (Wynn et al., 1991), interferon regulatory factor-1 (*IRF-1*) (Sims et al., 1993), and IFNγ-induced protein-10 (*IP-10*) (Luster et al., 1985) were analyzed. Seventy-two hours postinfection, immunohistochemical examination of MHC class II did not show differences in the expression pattern of class II molecules. Granulomatous lesions of *TRp55*$^{-/-}$ and control mice contained mainly class II–positive cells ($n = 3$ per group; data not shown). Also, throughout the liver parenchyma, comparable numbers of MHC class II–positive cells were found (data not shown). This indicates that in vivo, MHC class II expression on monocytes or macrophages and Kupffer cells is not impaired in the absence of TRp55. Twenty-four hours postinfection, the mRNAs for *mag-1*, *IRF-1*, and *IP-10* were readily induced in *TRp55*$^{-/-}$ mice as well as in control mice (Figure 5C). In summary, IFNγ receptor–mediated cellular responses appear not to be affected by the lack of TRp55 during an in vivo infection.

Up-Regulation of iNOS and Production of RNI

RNI have been implicated as mediators of antibacterial defense (Beckerman and al., 1993; MacMicking et al., 1995). In vitro, TNFα was described as directly inducing iNOS in synergy with IFNγ (Ding et al., 1988). A defect in an antibacterial mechanism in *TRp55*$^{-/-}$ mice thus might be the failure of iNOS transcription, which in turn leads to a deficiency in RNI production. Therefore, in a first approach, the capacity of thioglycollate-elicited *TRp55*$^{-/-}$ and *TRp55*$^{+/+}$ peritoneal exudate cells (PECs) for RNI production was tested. PEC were stimulated with murine TNFα and/or IFNγ and, as a control, with lipopolysaccharide (LPS) (Figure 6D). Culture supernatants were analyzed for the presence of NO metabolites using the Griess reagent (Green et al., 1982). After stimulation with LPS, PEC cultures from *TRp55*$^{-/-}$ and control mice contained comparable amounts of RNI, whereas stimulation with IFNγ alone was inefficient for generation of RNI (Figure 6D). As described before (Ding et al.,

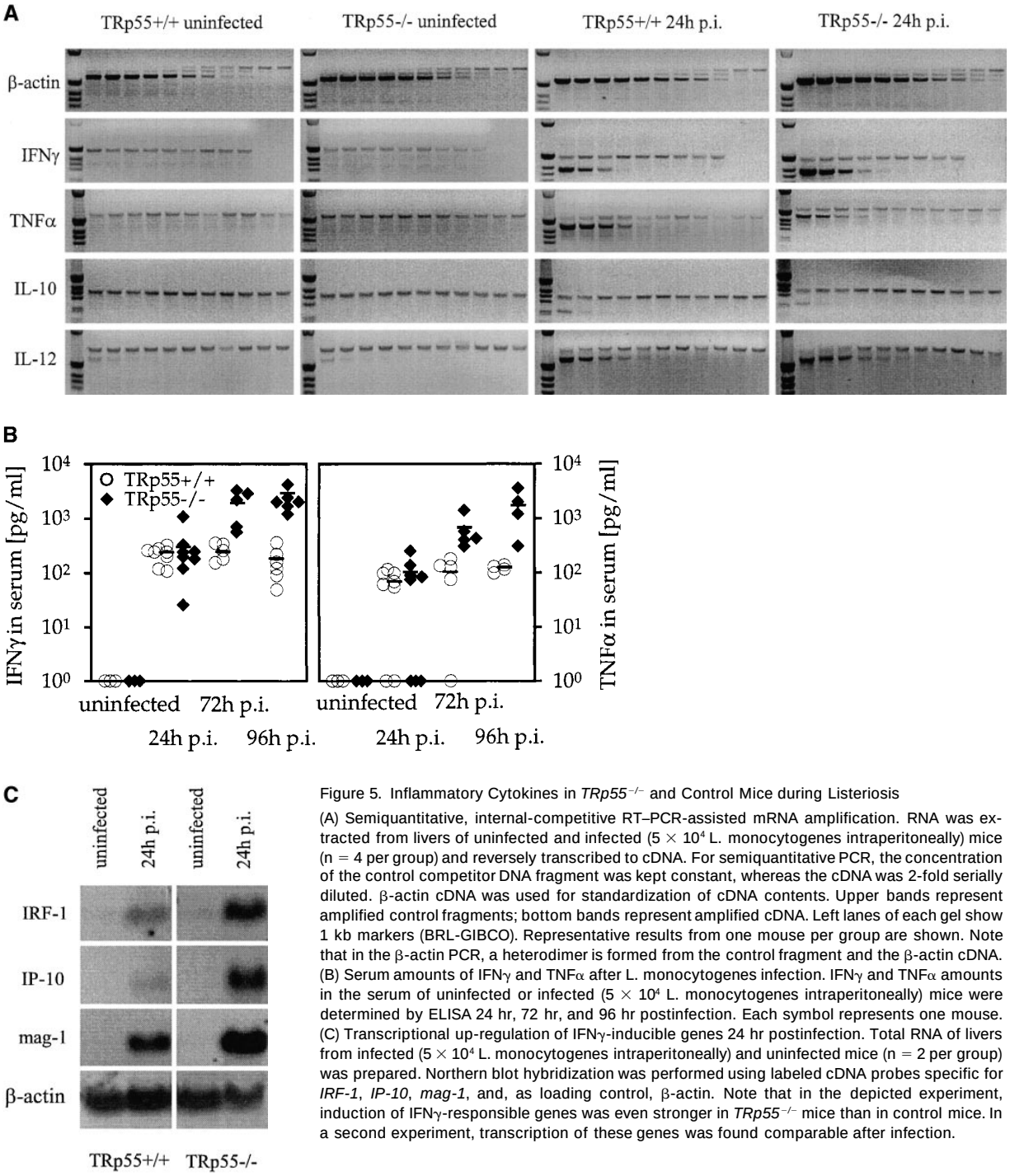

Figure 5. Inflammatory Cytokines in *TRp55$^{-/-}$* and Control Mice during Listeriosis

(A) Semiquantitative, internal-competitive RT–PCR-assisted mRNA amplification. RNA was extracted from livers of uninfected and infected (5×10^4 L. monocytogenes intraperitoneally) mice (n = 4 per group) and reversely transcribed to cDNA. For semiquantitative PCR, the concentration of the control competitor DNA fragment was kept constant, whereas the cDNA was 2-fold serially diluted. β-actin cDNA was used for standardization of cDNA contents. Upper bands represent amplified control fragments; bottom bands represent amplified cDNA. Left lanes of each gel show 1 kb markers (BRL-GIBCO). Representative results from one mouse per group are shown. Note that in the β-actin PCR, a heterodimer is formed from the control fragment and the β-actin cDNA.

(B) Serum amounts of IFNγ and TNFα after L. monocytogenes infection. IFNγ and TNFα amounts in the serum of uninfected or infected (5×10^4 L. monocytogenes intraperitoneally) mice were determined by ELISA 24 hr, 72 hr, and 96 hr postinfection. Each symbol represents one mouse.

(C) Transcriptional up-regulation of IFNγ-inducible genes 24 hr postinfection. Total RNA of livers from infected (5×10^4 L. monocytogenes intraperitoneally) and uninfected mice (n = 2 per group) was prepared. Northern blot hybridization was performed using labeled cDNA probes specific for *IRF-1*, *IP-10*, *mag-1*, and, as loading control, β-actin. Note that in the depicted experiment, induction of IFNγ-responsible genes was even stronger in *TRp55$^{-/-}$* mice than in control mice. In a second experiment, transcription of these genes was found comparable after infection.

1988), *TRp55$^{+/+}$* PECs cultured in the presence of TNFα and IFNγ readily produced RNI (Figure 6D). In marked contrast, PECs derived from *TRp55$^{-/-}$* mice could not be stimulated to produce RNI in response to TNFα and IFNγ (Figure 6D). This clearly indicates that TRp55-mediated signals are required synergistically with IFNγ-receptor signals for NO production in this in vitro situation.

After obtaining these in vitro findings, we studied the production of RNI during listeriosis in vivo. To this end, mRNA from livers of uninfected and infected *TRp55$^{-/-}$* and control mice was isolated, and cDNA was prepared. Total cDNA amounts were equilibrated by quantitation of β-actin cDNA using the internal-competitive PCR approach. Then, titrated aliquots of cDNAs were amplified with primers specific for iNOS. As expected, uninfected mice did not transcribe iNOS mRNA (Figure 6A). Twenty-four hours and 72 hr postinfection, substantial amounts of iNOS mRNA could be found in control mice; surprisingly however, comparable amounts of iNOS mRNA were also detected in *TRp55$^{-/-}$* livers. Moreover, immunohistochemical staining revealed the presence of iNOS

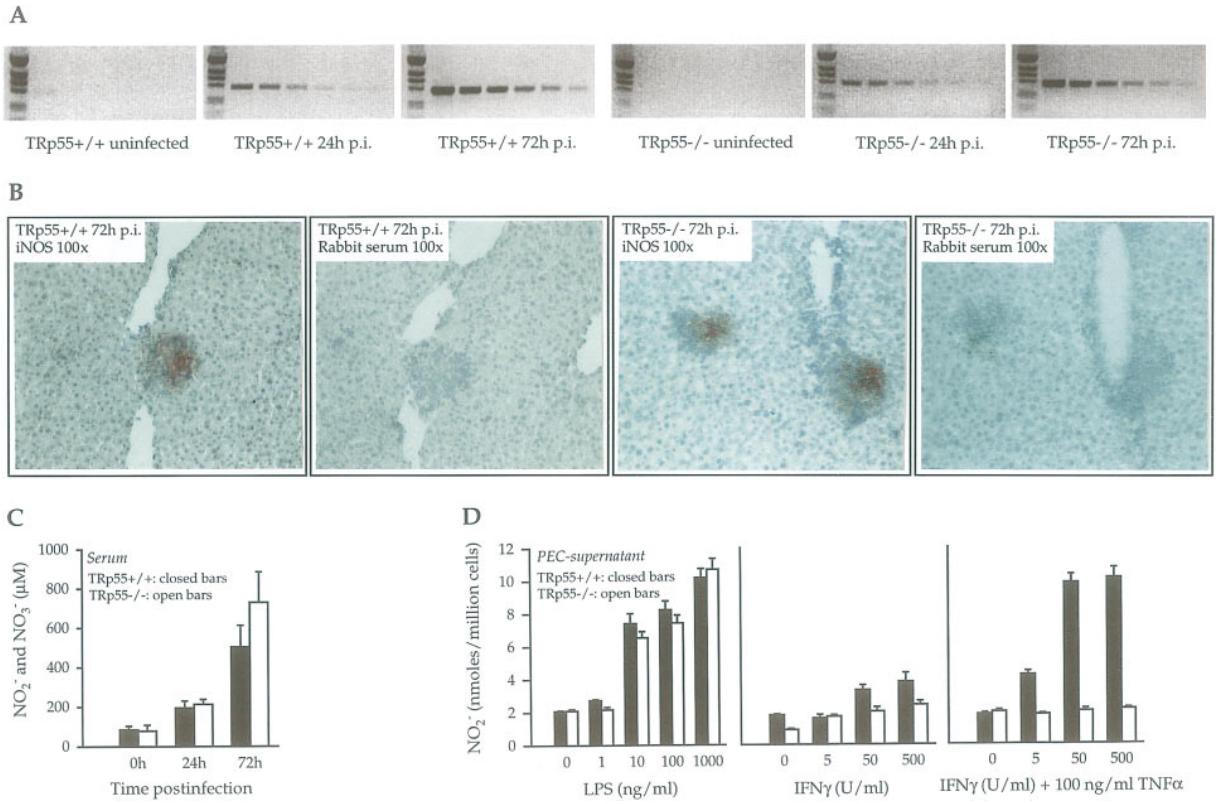

Figure 6. Up-Regulation of (A) iNOS mRNA in Livers, (B) iNOS Protein in Liver Granulomatous Lesions, (C) RNI Amounts in Serum, and (D) RNI Amounts in Supernatants of Cultured PEC

Mice were infected with 5×10^4 L. monocytogenes intraperitoneally or left untreated.

(A) Livers were removed 24 hr or 72 hr postinfection, and cDNA was prepared. Amounts of cDNA were standardized, employing an internal-competitive β-actin RT–PCR (not shown). Subsequently, amounts of iNOS mRNA were determined by performing RT–PCR on the 2-fold serially diluted, equilibrated cDNA (n = 3 per group; representative RT–PCR results from one mouse per group are shown).

(B) Immunohistological detection of iNOS protein in liver granulomatous lesions of mice 72 hr postinfection. Control sections were incubated with normal rabbit serum instead of the polyclonal anti-iNOS immune serum (n = 4 per group; representative sections are shown).

(C) Concentrations of RNI in serum of mice at indicated time points. Amounts of RNI were determined as previously described (Florquin et al., 1994) (n = 4 per group; mean ± SD).

(D) Concentrations of RNI in culture supernatants of thioglycollate-elicited PEC 24 hr after incubation of triplicate cultures with LPS, murine IFNγ, or a combination of murine IFNγ and murine TNFα. Representative results of one of five experiments are shown.

protein in cells within granulomatous lesions of homozygous-mutant and control mice (Figure 6B). These data were further verified by measurements of RNI in serum during the course of infection, demonstrating the presence of RNI metabolites in *TRp55*$^{-/-}$ and control mice (Figure 6C). Taken together, these results indicate first, that iNOS is transcribed, translated, and biologically active during L. monocytogenes infection; second, that TRp55-mediated up-regulation of iNOS can be replaced by other signal events in vivo; and third, even more important, that despite the presence of RNI, *TRp55*-deficient phagocytes are not capable of eliminating L. monocytogenes.

Necrotizing Pancreatitis in *TRp55*$^{-/-}$ Mice

Despite appropriate expression of inflammatory cytokines and the production of ROI and RNI at the places of infection, *TRp55*$^{-/-}$ mice ultimately succumb to L. monocytogenes infection. To investigate which organ system is damaged in L. monocytogenes infection, a systematic histopathological examination of several organs was performed. *TRp55*$^{-/-}$ and control mice were inoculated with 5×10^4 L. monocytogenes organisms, and hematoxylin–eosin and TUNEL (TdT-mediated dUTP-biotin nick end labeling) staining were carried out. Throughout the complete time course of infection, the majority of hepatocytes remained morphologically intact, and no significant increase in apoptosis could be detected outside granulomatous lesions (data not shown). This makes general liver failure as a potential cause of death very unlikely. No severe pathological defects were observed in the brain, meninges, lungs, heart, and kidneys (data not shown). Ninety-six hours postinfection, in crypts of the small intestine, increased numbers of apoptotic epithelial cells were found both in homozygous-mutant and control mice, whereas only in *TRp55*$^{-/-}$ mice, spleen cellularity and organization were disturbed by a massive, phagocytic infiltrate (data not shown). Unexpectedly, the most severe pathological finding was observed in the pancreas 96 hr postinfection. In marked contrast to control mice, up to one fourth of exocrine pancreatic cells in *TRp55*$^{-/-}$ mice revealed the morphological hallmarks of programmed cell death characterized by eosinophilia, cellular edema, pyknosis of nuclei,

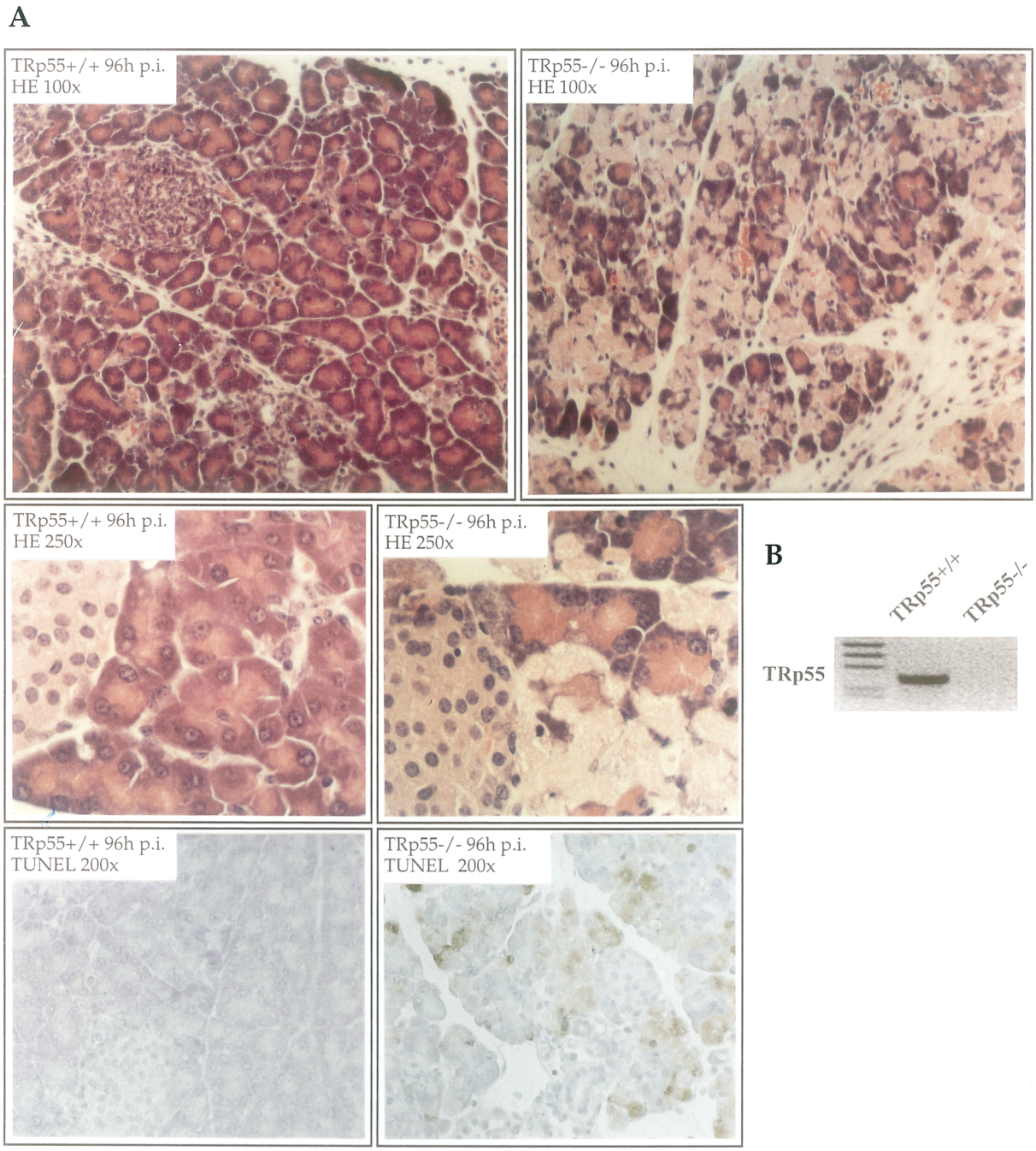

Figure 7. Pathohistological Analysis of the Pancreas and Expression of *TRp55* in Pancreatic Tissue

(A) Mice (n = 6 per group) were infected with 5×10^4 L. monocytogenes intraperitoneally, and after 96 hr, the pancreas was removed. Hematoxylin and eosin stainings and TUNEL reactions were performed on paraffin sections. For genotype of mice, stainings, and original magnifications, refer to inserts.

(B) Total pancreatic RNA was prepared from uninfected *TRp55*$^{-/-}$ and control mice. TRp55 mRNA was amplified by RT–PCR. Left lane: 1 kb marker (BRL-GIBCO); middle lane: control mice; right lane: *TRp55*$^{-/-}$ mice. Size of PCR product: 257 bp.

and karyorhexis, accompanied by the absence of an inflammatory reaction around dead cells (Figure 7A). Cell death was also observed distant from inflammatory foci, and in control mice, despite the presence of inflammatory foci, apoptotic cell death of pancreatic cells could not be found (Figure 7A). Of note, the endocrine pancreatic islets of Langerhans were completely spared from these alterations. TUNEL staining further corroborated these findings (Figure 7A). Some foci of fat necrosis in the peripancreatic tissue were found in *TRp55*$^{-/-}$ mice. Immunohistochemical staining of L. monocytogenes indicated that the majority of L. monocytogenes were colocalized with inflammatory cells in interlobular septs of the pancreatic gland or in inflammatory foci

(data not shown). RT–PCR of pancreatic tissue verified that the TRp55 is expressed in the pancreas of wild-type mice (Figure 7B). In summary, the histopathological analysis suggests that in the course of listeriosis, shortly before death, *TRp55*$^{-/-}$ animals suffer from an acute, necrotizing pancreatitis.

Discussion

TRp55$^{-/-}$ mice readily succumb to infection by intracellular bacteria such as L. monocytogenes or mycobacteria (Pfeffer et al., 1993; Rothe et al., 1993; Flynn et al., 1995). Surprisingly, the defense mechanisms that are defective in the absence of TNF or the TRp55 remain elusive. Here, evidence is provided that *TRp55*-deficient phagocytes, despite being recruited into infected tissues, are substantially compromised in their ability to eradicate L. monocytogenes. The failure to curb L. monocytogenes replication in vivo cannot be attributed to defective ROI or RNI production nor to failure of NK cell activation as characterized by IFNγ synthesis. The systematic investigation of pathological alterations in *TRp55*$^{-/-}$ mice revealed that the uncontrolled replication of L. monocytogenes finally resulted in the occurrence of acute pancreatitis with apoptosis of exocrine gland acini.

Emphasis in this study was laid upon direct investigation of all host responses in vivo. The importance of this approach can be best exemplified by the measurement of NO production in this study. The in vitro assay employing PECs might suggest that the TRp55 plays a limiting role for iNOS up-regulation; however, the direct ex vivo data indicate that TRp55 signals are not essential for production of NO during listeriosis. Thus, conclusions reached previously from correlating in vitro measurements of RNI and ROI to an observed phenotype such as susceptibility to listeriosis should be reviewed by direct in vivo experiments.

TRp55$^{-/-}$ mice are extremely susceptible to L. monocytogenes infection, and even minute amounts of bacteria cannot be controlled in these mice. This is in accordance with previously published data (Rothe et al., 1993). The major target organs of L. monocytogenes do not appear to be different between *TRp55*$^{-/-}$ and control mice, with spleen and liver containing vast numbers of bacteria. Interestingly, the pancreatic tissue also harbors many L. monocytogenes during the initial phase of infection, whereas in brain and meninges, recovery of L. monocytogenes is low. Infection studies with T cell– and B cell–deficient mice with severe combined immunodeficiency revealed that these mice can control L. monocytogenes replication as efficiently as wild-type mice within the first 4 days of infection (Bancroft et al., 1991). Thus, in *TRp55*$^{-/-}$ mice, the uncurbed bacterial growth within the first 4 days of infection and the early death indicate that a failure of innate immune responses and not of adaptive immune responses is detrimental for these animals.

The process of host resistance in murine listeriosis is multistaged. During the innate phase, several cell types such as granulocytes, macrophages, and NK cells as well as key cytokines such as IL-12, IFNγ, and TNFα are responsible for coping with these bacteria (Harty and Bevan, 1995; Unanue, 1997). To clarify which host processes fail in *TRp55*$^{-/-}$ mice during listeriosis, the recruitment of inflammatory cells and local in situ cytokine production were investigated. From the evidence provided here, it appears that the influx of granulocytes and of monocytes or macrophages recruited from the peripheral blood into infected tissues is not severely impeded in *TRp55*$^{-/-}$ mice. Also, formation of granulomatous lesions takes place in the absence of TRp55. Thus, expression of crucial adhesion molecules required for the early recruitment of inflammtory infiltrates is not significantly impaired in *TRp55*$^{-/-}$ animals during listeriosis. However, the presence of ultrastructurally intact L. monocytogenes in *TRp55*-deficient phagocytes accompanied by the evasion of L. monocytogenes from phagosomes and the infection studies on BM chimeras prove the marked inability of recruited phagocytes to kill L. monocytogenes organisms effectively. Previous studies indicate that IFNγ is one of the essential stimulators of macrophage listericidal activity (Buchmeier and Schreiber, 1985; Portnoy et al., 1989) and therefore is crucial for survival of L. monocytogenes infection (Huang et al., 1993; Harty and Bevan, 1995). In an in vitro model, NK cells from mice with severe combined immunodeficiency have been shown to be activated to produce IFNγ by macrophage-derived IL-12 and TNFα (Tripp et al., 1993, 1994). However, direct ex vivo evidence provided by semiquantitative PCR and ELISA in this study excludes the possibility that a defective production of phagocyte-activating cytokines such as IL-1β, IL-12, and IFNγ occurs in *TRp55*$^{-/-}$ mice. Also, the production of a macrophage-deactivating cytokine (IL-10) is not deregulated in *TRp55*$^{-/-}$ animals. These data indicate that TRp55 signals are not essential for the primary activation of NK cells to secrete IFNγ; however, it might be speculated that IFNγ production is regulated via TRp75 or, alternatively, that TNFα can be replaced for NK cell–dependent IFNγ secretion in vivo by other cytokines or signals such as IFNγ inducing factor (Okamura et al., 1995). Moreover, the lack of TRp55 in vivo does not hamper IFNγ receptor–mediated signals since transcriptional up-regulation of *mag-1*, *IRF-1*, and *IP-10* can be readily observed. Thus, a secondary defect due to a lack of IFNγ receptor–mediated signals appears to be an unlikely reason for the impaired host resistance of *TRp55*$^{-/-}$ mice.

It has been controversial as to whether RNI and ROI play pivotal roles in the resolution of murine L. monocytogenes infections (Beckerman et al., 1993; Gregory et al., 1993; Leenen et al., 1994; MacMicking et al., 1995; Dramsi et al., 1996; Fehr et al., 1997). Here, we show that absence of ROI leads to an only slightly increased susceptibility, whereas absence of TRp55 has a profound effect on the outcome of an L. monocytogenes infection. Moreover, *TRp55*-deficient as well as wild-type granulocytes responded in a comparable way with an increased oxidative burst formation after infection. Taking into account that in vivo generation of RNI also takes place in *TRp55*$^{-/-}$ mice, it can be concluded that, surprisingly, in vivo production of neither RNI nor of ROI plays a decisive role in the antilisterial activity of phagocytes. Further analysis revealed that lysozyme M

mRNA was comparably expressed in *TRp55$^{-/-}$* and control mice (data not shown). Other bactericidal mechanisms such as defensins and the action of NRAMP1 (natural resistance-associated macrophage protein 1) are not likely to contribute significantly to resistance against listeriosis since defensins have so far not been found in murine neutrophils (Ganz and Lehrer, 1994), and NRAMP1 is defective in the C57BL/6 background used, in which a natural mutation renders this protein nonfunctional, respectively (Vidal et al., 1995). In vitro reports about iron metabolism of PECs suggested that limitation of intracellular iron may lead to increased resistance to L. monocytogenes by direct interference with the essential bacterial iron metabolism (Alford et al., 1991). Also, phagosome acidification plus phagosome–lysosome fusion plays a role in antibacterial defense (Kaufmann, 1993). Whether TRp55-mediated signals lead, first, to enhancement of iron-binding proteins, second, to acidification of vacuolar compartments, or, third, to the induction of a yet unknown bactericidal effector function remains to be investigated. In this regard, it is noteworthy that NF-IL-6, a transcription factor known to be induced by TNFα (Akira et al., 1995), is involved in anti–L. monocytogenes defense. Similar to *TRp55$^{-/-}$* mice, NF-IL-6–deficient mice are highly susceptible to L. monocytogenes infection (Tanaka et al., 1995). Thus, it is intriguing to speculate on the existence of an unknown bactericidal system that is under the control of both TRp55-signaling and NF-IL-6 transactivation.

Recently, it has been suggested that TNFα might be needed for lysis of infected hepatocytes, thereby making L. monocytogenes accessible for elimination by neutrophils and/or macrophages (Portnoy, 1992). However, our data, consistent with recent in vitro findings (Rogers et al., 1996), do not lend in vivo support to the hypothesis of a role for TRp55 on hepatocytes during listeriosis: first, C57BL/6 BM→*TRp55$^{-/-}$* chimeras are relatively resistant to listeriosis, although these animals lack the TRp55 on all hepatocytes. Second, 3 days postinfection, the majority of L. monocytogenes are colocalized with phagocytes inside granulomatous lesions, suggesting that lysis of primarily infected hepatocytes must have occurred appropriately up to this time point. The presence of heavily infected hepatocytes at the periphery of granulomatous lesions after 96 hr may be explained by a secondary infection by L. monocytogenes now spreading from infected phagocytes inside granulomatous lesions to neighboring hepatocytes. Surprisingly, the systematic pathohistological examination of all parenchymal organs of L. monocytogenes–infected animals revealed that *TRp55$^{-/-}$* mice suffer from necrotizing pancreatitis, with significant cell death limited to the exocrine part of the gland. Other tissues, especially the liver parenchyma outside granulomatous lesions and the brain, do not show significantly increased numbers of apoptotic cells. Apoptotic cell death of exocrine pancreatic cells can be envisaged to occur as a result of direct infection with L. monocytogenes. However, as the vast majority of L. monocytogenes are colocalized with recruited inflammatory cells in the pancreatic septae, and since apoptotic areas inside exocrine lobules could be also observed far away from inflammatory cells (Figure 7A), it appears unlikely that all pancreatic cells were directly infected and lysed by L. monocytogenes. Another interesting hypothesis might be that in the late stage of disease, the lack of the TRp55 renders exocrine pancreatic cells prone to apoptosis induced by stress, such as a reduced oxygen supply or high concentrations of harmful granulocyte products and bacterial toxins. In vitro, nuclear translocation of NF-κB species containing relA (p65) has been shown to protect cell lines from programmed cell death induced by ionizing radiation or treatment with daunorubicin (Wang et al., 1996). In pancreatic tissue of wild-type mice, TRp55 is expressed (Figure 7B). Thus, anti-apoptotic signals might be mediated by the potent, TRp55-induced activation of NF-κB. Yet, regardless of the pathogenesis, it is a well-documented clinical observation in humans that acute pancreatitis can cause a severe, sometimes lethal shock syndrome (Wilson and Imrie, 1988; Steinberg and Tenner, 1994). By analogy, the occurrence of a necrotizing pancreatitis may also contribute to the development of a lethal shock syndrome in *TRp55$^{-/-}$* animals.

In summary, *TRp55$^{-/-}$* mice prove to be extremely valuable tools for dissecting the innate host defense mechanisms responsible for the highly effective initial control of L. monocytogenes replication.

Experimental Procedures

Mice and Bacteria

The following mice, 8–12 weeks old, were used: *TRp55$^{-/-}$* mice on a C57BL/6 background (Pfeffer et al., 1993), *p47$^{phox-/-}$* mice on a C57BL/6 × Sv129 background (Jackson et al., 1995), and corresponding control mice. Overnight cultures of L. monocytogenes (American type culture collection strain 43251) were grown in brain–heart infusion (Difco, Detroit), adjusted to an optical density of 0.75 and serially diluted in medium. Titrated numbers of L. monocytogenes were inoculated in a volume of 500 μl intraperitoneally into the mice. The dose of bacteria was checked by plating 10 μl aliquots of a serial 10-fold dilution on Columbia blood agar plates and counting the colony forming units after overnight incubation at 37°C. Livers from infected mice were removed at different time points after L. monocytogenes inoculation; organ homogenates were prepared; and bacterial counts were determined as above.

Antibodies

The following rat monoclonal antibodies were used for immunohistochemistry or flow cytometry (the recognized murine antigens are given in parentheses): M1/70 (Mac-1), RB6-8C5 (Gr-1), F4/80 (F4/80), GK-1.5 (L3T4), 53672 (Lyt2), Ox-7 (Thy1.1), 53-2.1 (Thy1.2), and Tib120 (I-A^{b,d,q}/I-E^{d,k}). All clones except RB6-8C5, Ox-7, and 53-2.1 were obtained as hybridomas from the American type culture collection (Rockville, MD). RB6-8C5, Ox-7 (fluorescein isothiocyanate–labeled), and 53-2.1 (phycoerythrin-labeled) were purchased from Pharmingen (Hamburg, Germany). The concentrations of antibodies in hybridoma supernatants or purifications were adjusted to 10 μg/ml. Polyclonal rabbit serums raised against a C-terminal peptide from murine iNOS (Biomol, Hamburg, Germany) and L. monocytogenes type 1 and 4 O- and H-antigens (Behring, Marburg, Germany), respectively, were used in a 1:10,000 dilution and a 1:5,000 dilution in phosphate-buffered saline (PBS), respectively, containing 5% (v/v) mouse serum and 1% (w/v) bovine serum albumin. Secondary polyclonal peroxidase-coupled antibodies were mouse F(ab′)$_2$ anti-rat IgG-Fc (Dianova, Hamburg, Germany) and goat anti-rabbit IgG-Fc (Biorad, Munich).

Immunohistochemistry

Tissue samples were snap-frozen in 2-methylbutane (Merck, Darmstadt, Germany) prechilled by liquid nitrogen. Cryostat sections (8 μm) were fixed for 10 min in ice-cold acetone (Merck) and dried. For reduction of unspecific background staining, sections used for

Table 2. Oligonucleotide Primers Used for Conventional or Semiquantitative RT–PCR Assays

β-actin (569 bp)	Sense	5′-ATGGATGACGATATCGCT-3′
	Antisense	5′-ATGAGGTAGTCTGTCAGGT-3′
IFNγ (388 bp)	Sense	5′-GAAAGCCTAGAAAGTCTGAATAACT-3′
	Antisense	5′-ATCAGCAGCGACTCCTTTTCCGCTT-3′
TNFα (456 bp)	Sense	5′-GACAAGCCTGTAGCCCACGTCGTAG-3′
	Antisense	5′-ACACCCATTCCCTTCACAGAGCAAT-3′
IL-10 (237 bp)	Sense	5′-ACCTGGTAGAAGTGATGCCCCAGGCA-3′
	Antisense	5′-CTATGCAGTTGATGAAGATGTCAAA-3′
IL-12 p40 (576 bp)	Sense	5′-CGTGCTCATGGCTGGTGCAAAG-3′
	Antisense	5′-GAACACATGCCCACTTGCTG-3′
TRp55 (257 bp)	Sense	5′-TCTCAGTTGCAAGACATGTCGG-3′
	Antisense	5′-AGTGGCTGCAAGGGACGCACTC-3′
Lysozyme M (448 bp)	Sense	5′-CATGAAGACTCTCCTGACTC-3′
	Antisense	5′-GGTCAGACTCCGCAGTTCCG-3′
iNOS (292 bp)	Sense	5′-CTACGTTCAGGACATCCTGC-3′
	Antisense	5′-TCAGAGCCTCGTGGCTTTGG-3′

The expected size of the amplified cDNA is given in parentheses.

detection of iNOS and L. monocytogenes were preincubated with 100 μl PBS containing 5% (v/v) mouse serum and 1% (w/v) bovine serum albumin for 45 min. All incubations were performed in a moist chamber at room temperature. Sections were then incubated for 45 min with 100 μl of the primary antibody, followed by three washes with PBS and addition of 100 μl of the peroxidase-coupled secondary antibody for 30 min. The sections were rinsed three times with PBS and stained with 5% (v/v) 5 mg/ml 3-aminoethylcarbazole (Sigma, Deisenhofen, Germany) in N,N′-dimethylformamide (Merck) and 0.01% (v/v) H_2O_2 (Merck) in 50 mM acetate buffer for 10 min. After washing in PBS (3×), the sections were counterstained with Mayer's hematoxylin (Sigma) for 10 min and mounted with glycerol–gelatin (Sigma). The stained sections were photographed using a Leica DMRBE photomicroscope (Leica Instruments, Nussloch, Germany).

Histology

Tissues were fixed in 10% buffered formaline and embedded in paraffin according to conventional procedures. Sections (5 μm) were stained with hematoxylin–eosin or by the TUNEL method (Gavrieli et al., 1992) using a kit from Boehringer, Mannheim, Germany. TUNEL reactions were carried out as described in the manufacturer's kit protocol.

Electron Microscopy

Liver tissue was fixed in 3% glutaraldehyde in 0.1 M sodium cacodylate buffer (pH 7.6). The glutaraldehyde fixed tissues were postfixed in Dalton's 1% osmium tetroxide. Ultrathin sections were stained with uranyl acetate and lead nitrate in a Leica ultrastainer and examined with a Zeiss EM 10 CR transmission electron microscope.

Radiation BM Chimeras

Recipient C57BL/6 and *TRp55*$^{-/-}$ mice bearing either the Thy1.1 or the Thy1.2 antigen on T cells were irradiated with 12 Gy using a ^{60}Co irradiator (Buchler, Braunschweig, Germany). BM was collected from the shafts of femurs and tibias of *TRp55*$^{-/-}$ (Thy1.2$^+$) or C57BL/6 (Thy1.1$^+$ or Thy1.2$^+$) donor mice. After washing, 1×10^6 BM cells were injected intravenously into recipients. Eight weeks later, the degree of chimerism was determined by flow cytometric analysis of the Thy1.1 and Thy1.2 antigen expression.

Oxidative Burst

Flow cytometric analysis of oxidative burst was adapted from Vowells et al. (1995). In brief, 150 μl of whole blood from naive or infected mice was collected, and erythrocytes were lysed for 5 min in 20 ml of prewarmed lysis buffer (pH 7.3) containing 0.83% (w/v) ammonium chloride, 0.168% (w/v) sodium bicarbonate, and 1 mM EDTA. The remaining leukocytes were washed once in 5 ml Hank's balanced salt solution (pH 7.3) without Ca^{2+}, Mg^{2+}, and phenol red, and then resuspended in 1 ml of this buffer. After incubation for 15 min with 160 μM dihydrorhodamine 123 (MoBiTec, Göttingen, Germany), sodium azide (2.5 μM) and cytochalasin B (0.05 mM; Serva, Heidelberg, Germany) were added. Cells were split and, first, mock stimulated with medium or, second, stimulated with 4 μM fMLP (Sigma) for 20 min at 37°C. Flow cytometric analysis of cells in the granulocyte gate was performed immediately afterward on an EPICS XL cytometer (Coulter Electronics, Krefeld, Germany). Dihydrorhodamine 123 is oxidized to rhodamine 123 in the presence of ROI such as H_2O_2 or O_2^-. Rhodamine 123 emits a bright fluorescent signal upon excitation at 488 nm that can be detected at 525 nm.

Purification of RNA, cDNA Synthesis, and Semiquantitative RT–PCR

Approximately 100 mg of tissue was homogenized in 3 ml of lysis buffer consisting of 4 M guanidinium thiocyanate (Merck), 0.5% (w/v) N-lauroyl-sarcosine (Serva, Germany), 15 mM Na^{2+}-citrate (pH 7.0), and 100 mM 2-mercaptoethanol (Sigma). Total RNA was prepared as described elsewhere (Chomczynski and Sacchi, 1987). Pancreatic tissue was first pulverized in liquid nitrogen before RNA preparation according to the above protocol was performed. RNA precipitates were then washed once in 75% ethanol, repelleted by centrifugation at 13,000 × g at 4°C, and dissolved in 100 μl of diethylpyrocarbonate-treated ddH_2O. Four micrograms of total RNA was incubated with 10 μM oligo-dT (12 to 18 mer; BRL-GIBCO, Berlin) and 10 μM random hexamer primer (BRL-GIBCO) in a 10 μl reaction mix at 65°C for 10 min. The reaction mixture was cooled on ice, and cDNA synthesis was carried out by adding 4 μl 5× transcription buffer (250 mM Tris-HCl, 375 mM KCl, 15 mM $MgCl_2$ [pH 8.3]; BRL-GIBCO), 2 μl 0.1 M dithiothreitol (BRL-GIBCO), 2 μl dNTP mix (final concentration: 1 mM each dNTP), 0.5 μl RNasin (15 U; Promega, Madison, WI), and 1 μl Moloney murine leukemia virus reverse transcriptase (200 U Superscript; BRL-GIBCO). The mixture was incubated for 60 min at 37°C and then heated to 95°C for 5 min. After cooling on ice, the 20 μl reaction mix was diluted with ddH_2O to 60 μl, and a 2-fold serial dilution was prepared. For semiquantitative PCR, 10 μl from each cDNA dilution were amplified in PCR reaction plates (Corning-Costar, Cambridge, MA) containing a known and constant amount of control DNA fragment; specific 5′ and 3′ primers (final concentrations: 200 nM); 200 μM dNTP; 5 U Taq-polymerase (BRL-GIBCO); and PCR buffer containing 500 mM KCl, 100 mM Tris-Cl (pH 8.3), 25 mM $MgCl_2$–6 H_2O, and 1% (w/v) gelatin. The PCR reaction was performed in a 96-well thermal cycler (Biometra, Göttingen, Germany) for 30 cycles with a 1 min denaturation step at 94°C; a 30 s annealing step at 63°C; and a 1 min, 30 s extension step at 72°C. Linear control DNA fragments were designed to be identical to the amplified specific cytokine cDNA except for the insertion of a 125 bp piece of unrelated β-actin DNA in the middle of the control fragments (H. N. and K. P., unpublished data). The sequences of sense and antisense primers used in this study are shown in Table 2. An internal-competitive PCR was performed using the titrated

cDNA and specific β-actin primers to allow standardization of the samples. The amount of β-actin cDNA was calculated from the dilution at which ethidium bromide stained bands of coamplified cDNA and control fragment showed equal density after electrophoresis. The specific cytokine cDNA amounts were determined in the same manner.

Measurements of IFNγ, TNFα, and IL-1β in the Serum

Mice were injected intraperitoneally with 50,000 L. monocytogenes, and sera were collected 1, 3, and 4 days later. Amounts of IFNγ, TNFα, and IL-1β in the sera of wild-type and homozygous-mutant mice were determined with murine IFNγ, TNFα, and IL-1β ELISA kits from Genzyme (Cambridge, MA). ELISAs were performed according to the manufacturer's protocol.

Northern Blot Hybridization

Liver RNA was isolated as described above, separated in a formaldehyde agarose gel, transferred to a GeneScreen Plus membrane (Biotechnology Systems, Boston), and probed with fluorescein-labeled cDNAs for *IRF-1*, *mag-1*, and *IP-10*. Methylene blue staining of the membrane and hybridization with labeled mouse β-actin cDNA were performed for loading control. Labeling of cDNAs and detection of hybridization products were carried out according to the manufacturer's protocol (Amersham, Little Chalfont, UK).

Measurement of Nitrite and Nitrate Amounts

Amounts of NO_2^- and NO_3^- in the serum were determined as described elsewhere (Florquin et al., 1994). NO_2^- amounts in the supernatants of cultured, thioglycollate-elicited PECs were measured as follows: 1 ml of 3% thioglycollate was injected intraperitoneally 5 days prior to cell harvest by peritoneal lavage with 10 ml of RPMI 1640 (Seromed, Berlin) supplemented with 10% (v/v) fetal calf serum (Seromed), 50 μg/ml streptomycin (Seromed), 50 μM 2-mercaptoethanol (BRL-GIBCO), and 2 mM glutamine (Seromed). PECs were washed once and allowed to adhere for 4 hr at 37°C onto 96-well plates at 3×10^5 cells/well. Wells were gently washed three times to remove nonadherent cells. PECs were stimulated with varying amounts of LPS (Sigma, catalog no. L-3129), murine IFNγ, and murine TNFα (both Genzyme) for 24 hr at 37°C. Finally, 50 μl of culture supernatant was mixed with 50 μl of Griess reagent (Green et al., 1982). The absorbance at 550 nm was measured in an ELISA reader, and NO^{2-} concentrations were calculated from an $NaNO_2$ (Sigma) standard curve.

Statistics

Statistical analysis of data was carried out using the Student's paired t test.

Acknowledgments

The authors thank U. Huffstadt, E. Schaller, K. Mink, and A. Nickl for expert technical help. For helpful scientific discussions and critical reading of the manuscript, the authors would like to thank M. Alimzhanov, H. Häcker, T. Plitz, S. Ehlers, and R. Schmid. This work was supported by Deutsche Forschungsgemeinschaft grant Pf 259/2–3, Klinische Forschergruppe "Immunsuppression und postoperative Sepsis" project B2, and SFB 391 project B3.

Received June 11, 1997.

References

Akira, S., Yoshida, K., Tanaka, T., Taga, T., and Kishimoto, T. (1995). Targeted disruption of the IL-6 related genes: gp130 and NF-IL6. Immunol. Rev. *148*, 221–253.

Alford, C.E., King, T.E., Jr., and Campbell, P.A.. (1991). Role of transferrin, transferrin receptors, and iron in macrophage listericidal activity. J. Exp. Med. *174*, 459–466.

Bancroft, G.J., Schreiber, R.D., and Unanue, E.R.. (1991). Natural immunity: a T-cell-independent pathway of macrophage activation, defined in the SCID mouse. Immunol. Rev. *124*, 5–24.

Beckerman, K.P., Rogers, H.W., Corbett, J.A., and Schreiber, R.D., McDaniel, M.L., and Unanue, E. (1993). Release of nitric oxide during the T cell-independent pathway of macrophage activation. J. Immunol. *150*, 888–895.

Bevilacqua, M.P. (1993). Endothelial-leukocyte adhesion molecules. Annu. Rev. Immunol. *11*, 767–804.

Buchmeier, N.A., and Schreiber,. R.D. (1985). Requirement of endogenous interferon-gamma production for resolution of Listeria monocytogenes infection. Proc. Natl. Acad. Sci. USA *82*, 7404–7408.

Chomczynski, P., and Sacchi, N. (1987). Single-step method of RNA isolation by acid guanidinium thiocyanate-phenol-chloroform extraction. Anal. Biochem. *162*, 156–159.

Clatham, W.W., Turkiewicz, A., and Blackburn, W.D., Jr. (1994). Determinants of neutrophil HOCl generation: ligand-dependent responses and the role of surface adhesion. J. Leukoc. Biol. *56,* 654–660.

Conlan, J.W., and North, R.J. (1991). Neutrophil-mediated dissolution of infected host cells as a defense strategy against a facultative intracellular bacterium. J. Exp. Med. *174*, 741–744.

Conlan, J.W., and North, R.J. (1994). Neutrophils are essential for early anti-Listeria defense in the liver, but not in the spleen or peritoneal cavity, as revealed by a granulocyte-depleting monoclonal antibody. J. Exp. Med. *179*, 259–268.

Ding, A.H., Nathan, C.F., and Stuehr, D.J. (1988). Release of reactive nitrogen intermediates and reactive oxygen intermediates from mouse peritoneal macrophages. J. Immunol. *141*, 2407–2412.

Dramsi, S., Leburn, M., and Cossart, P. (1996). Molecular and genetic determinants involved in invasion of mammalian cells by *Listeria monocytogenes*. Curr. Top. Microbiol. Immunol. *209*, 61–77.

Dunn, P.L., and North, R.J. (1991). Early gamma interferon production by natural killer cells is important in defense against murine listeriosis. Infect. Immun. *59*, 2892–2900.

Fehr, T., Schoedon, G., Odermatt, B., Holtschke, T., Schneemann, M., Bachmann, M.F., Mak, T.W., Horak, I., and Zinkernagel, R.M. (1997). Crucial role of interferon consensus sequence binding protein, but neither of interferon regulatory factor 1 nor of nitric oxide synthesis for protection against murine listeriosis. J. Exp. Med. *185*, 921–932.

Florquin, S., Amraoui, Z., Dubois, C., Decuyper, J., and Goldman, M. (1994). The protective role of endogenously synthesized nitric oxide in staphylococcal enterotoxin B-induced shock in mice. J. Exp. Med. *180*, 1153–1158.

Flynn, J.L., Goldstein, M.M., Chan, J., Thiebold, K.J., Pfeffer, K., Lowenstein, C.J., Schreiber, R., Mak, T.W., and Bloom, B.R. (1995). Tumor necrosis factor-α is required in the protective immune response against Mycobacterium tuberculosis in mice. Immunity *2*, 561–572.

Ganz, T., and Lehrer, R.I. (1994). Defensins. Curr. Opin. Immunol. *6*, 584–589.

Gavrieli, Y., Sherman, Y., and Ben-Sasson, S.A. (1992). Identification of programmed cell death in situ via specific labeling of nuclear DNA fragmentation. J. Cell Biol. *119*, 493–501.

Goosens, P.L., Juin, H., and Milon, G. (1991). Dynamics of lymphocytes and inflammatory cells recruited in liver during murine listeriosis. J. Immunol. *147*, 3514–3520.

Green, K., Wagner, D., Glogowski, J., Skipper, P., Wishnok, J., and Tannenbaum, S. (1982). Analysis of nitrate, nitrite and [^{15}N] nitrate in biological fluids. Anal. Biochem. *126*, 131–138.

Gregory, S.H., Wing, E.J., Hoffmann, R.A., and Simmons, R.L. (1993). Reactive nitrogen intermediates suppress the primary immunologic response to *Listeria*. J. Immunol. *150*, 2901–2909.

Harty, J.T., and Bevan, M.J. (1995). Specific immunity to Listeria monocytogenes in the absence of IFNγ. Immunity *3*, 109–117.

Harty, J.T., Lenz, L.L., and Bevan, M.J. (1996). Primary and secondary immune responses to *Listeria monocytogenes*. Curr. Opin. Immunol. *8*, 526–530.

Havell, E.D. (1989). Evidence that tumor necrosis factor has an important role in antibacterial resistance. J. Immunol. *143*, 2894–2899.

Huang, S., Hendriks, W., Althage, A., Hemmi, S., Bluethmann, H., Kamijo, R., Vilcek, J., Zinkernagel, R.M., and Aguet, M. (1993). Immune response in mice that lack the interferon-gamma receptor. Science *259*, 1742–1745.

Jackson, S.H., Gallin, J.I., and Holland, S.M. (1995). The p47^{phox} mouse knock-out model of chronic granulomatous disease. J. Exp. Med. *185*, 751–758.

Kaufmann, S.H.E. (1993). Immunity to intracellular bacteria. Annu. Rev. Immunol. *11*, 129–163.

Kindler, V., Sappino, A.-P., Grau, G.E., Piguet, P.-F., and Vassalli, P. (1989). The inducing role of tumor necrosis factor in the development of bactericidal granulomas during BCG infection. Cell *56*, 731–740.

Leenen, P.J.M., Canono, B.P., Drevets, D.A., Voerman, J.S.A., and Campell, P.A. (1994). TNF-α and IFN-γ stimulate a macrophage precursor cell line to kill *Listeria monocytogenes* in a nitric oxide–independent manner. J. Immunol. *153*, 5141–5147.

Lepay, D.A., Steinman, R.M., Nathan, C.F., Murray, H.W., and Cohn, Z.A. (1985). Liver macrophages in murine listeriosis. J. Exp. Med. *161*, 1503–1512.

Luster, A.D., Unkeless, J.C., and Ravetch, J.V. (1985). γ-Interferon transcriptionally regulates an early response gene containing homology to platelet proteins. Nature *315*, 672–676.

MacMicking, J.D., Nathan, C., Hom, G., Chartrain, N., Fletcher, D.S., Trumbauer, M., Stevens, K., Xie, Q.-w., Sokol, K., Hutchinson, N., et al. (1995). Altered responses to bacterial infection and endotoxic shock in mice lacking inducible nitric oxide synthase. Cell *81*, 641–650.

Mandel, T.F., and Cheers, C. (1980). Resistance and susceptibility of mice to bacterial infection: histopathology of listeriosis in resistant and susceptible strains. Infect. Immun. *30* 851–861.

Nakane, A., Minagawa, T., and Kato, K. (1988). Endogenous tumor necrosis factor (cachectin) is essential to host resistance against *Listeria monocytogenes* infection. Infect. Immun. *56*, 2563–2569.

Neumann, B., Machleidt, T., Lifka, A., Pfeffer, K., Vestweber, D., Mak, T.W., Holzmann, B., and Krönke, M. (1996). Crucial role of 55-kilodalton TNF receptor in TNF-induced adhesion molecule expression and leukocyte organ infiltration. J. Immunol. *156*, 1587–1593.

Okamura, H., Tsutsui, H., Komatsu, T., Yutsudo, M., Hakura, A., Tanimoto, T., Torigoe, K., Okura, T., Nukada, Y., Hattori, K., et al. (1995). Cloning of a new cytokine that induces IFN-gamma production by T-cells. Nature *378*, 88–91.

Peck, R. (1989). Gamma interferon induces monocyte killing of *Listeria monocytogenes* by an oxygen-dependent pathway; alpha- or beta-interferons by oxygen-independent pathways. J. Leukoc. Biol. *46*, 434–440.

Pfeffer, K., Matsuyama, T., Kündig, T.M., Wakeham, A., Kishihara, K., Shahinian, A., Wiegmann, K., Ohashi, P.S., Krönke, M., and Mak, T.W. (1993). Mice deficient for the 55 kd tumor necrosis factor receptor are resistant to endotoxic shock, yet succumb to L. monocytogenes infection. Cell *73*, 457–467.

Portnoy, D.A. (1992). Innate immunity to a facultative intracellular bacterial pathogen. Curr. Opin. Immunol. *4*, 20–24.

Portnoy, D.A., Schreiber, R.D., Connelly, P., and Tilney, L.G. (1989). γ Interferon limits access of *Listeria monocytogenes* to the macrophage cytoplasm. J. Exp. Med. *170*, 2141–2145.

Racz, P., Tenner, K., and Merö, M. (1970). Electron microscopic studies in experimental keratoconjunctivitis listeriosa. I. Penetration of Listeria monocytogenes into corneal epithelial cells. Acta Microbiol. Acad. Sci. Hung. *17*, 221–236.

Rogers, H.W., and Unanue, E.R. (1993). Neutrophils are involved in acute, non-specific resistance to *Listeria monocytogenes* in mice. Infect. Immun. *61*, 5090– 5096.

Rogers, H.W., Callery, M.P., Deck, B., and Unanue, E.R. (1996). *Listeria monocytogenes* induces apoptosis of infected hepatocytes. J. Immunol. *156*, 679–684.

Rosen, H., Gordon, S., and North, R.J. (1989). Exacerbation of murine listeriosis by a monoclonal antibody specific for the type 3 complement receptor of myelomonocytic cells. J. Exp. Med. *170*, 27–37.

Rothe, J., Lesslauer, W., Lötscher, H., Lang, Y., Koebel, P., Köntgen, F., Althage, A., Zinkernagel, R., Steinmetz, M., and Bluethmann, H. (1993). Mice lacking the tumour necrosis factor receptor 1 are resistant to TNF-mediated toxicity but highly susceptible to infection by Listeria monocytogenes. Nature *364*, 798–802.

Sims, S.H., Cha, Y., Romine, M.F., Gao, P.Q., Gottlieb, K., Deisseroth, A.B. (1993). A novel interferon-inducible domain: structural and functional analysis of the human interferon regulatory factor 1 gene promoter. Mol. Cell. Biol. *13*, 690–702.

Steinberg, W., and Tenner, S. (1994). Acute pancreatitis. N. Engl. J. Med. *330*, 1198–1210.

Tanaka, T., Akira, S., Yoshida, K., Umemoto, M., Yoneda, Y., Shirafuji, N., Fujiwara, H., Suematsu, S., Yoshida, N., and Kishimoto, T. (1995). Targeted disruption of the NF-IL6 gene discloses its essential role in bacteria killing and tumor cytotoxicity by macrophages. Cell *80*, 353–361.

Teixeira, H.C., and Kaufmann, S.H.E. (1994). Role of NK1.1+ cells in experimental listeriosis. J. Immunol. *152*, 1873–1882.

Tripp, C.S., Wolf, S.F., and Unanue, E.R. (1993). Interleukin 12 and tumor necrosis factor α are costimulators of interferon γ production by natural killer cells in severe combined immunodeficiency mice with listeriosis, and interleukin 10 is a physiologic antagonist. Proc. Natl. Acad. Sci. USA *90*, 3725–3729.

Tripp, C.S., Gately, M.K., Hakimi, J., Ling, P., and Unanue, E.R. (1994). Neutralization of IL-12 decreases resistance to Listeria in SCID and C.B-17 mice. J. Immunol. *152*, 1883–1887.

Unanue, E.R. (1997). Inter-relationship among macrophages, natural killer cells and neutrophils in early stages of *Listeria* resistance. Curr. Opin. Immunol. *9*, 35–43.

Vidal, S., Tremblay, M.L., Govoni, G., Gauthier, S., Sebastiani, G., Malo, D., Skamene, E., Olivier, M., Jothy, S., and Gros, P. (1995). The *Ity/Lsh/Bcg* locus: natural resistance to infection with intracellular parasites is abrogated by disruption of the *NRAMP1* gene. J. Exp. Med. *182*, 655–666.

Vowells, S.J., Sekhsaria, S., Malech, H.L., Shalit, M., and Fleischer, T.A. (1995). Flow cytometric analysis of the granulocyte respiratory burst: a comparison study of fluorescent probes. J. Immunol. Methods *178*, 89–97.

Wang, C.-Y., Mayo, M.W., and Baldwin, A.S., Jr. (1996). TNF- and cancer therapy–induced apoptosis: potentiation by inhibition of NF-κB. Science *274*, 784–787.

Wilson, C., and Imrie, C.W. (1988). Deaths from acute pancreatitis: why do we miss the diagnosis so frequently? Int. J. Pancreatol. *3*, 273–281.

Wynn, T.A., Nicolet, C.M., and Paulnock, D.M. (1991). Identification and characterization of a new gene family induced during macrophage activation. J. Immunol. *147*, 4384–4392.